



Physics-informed neural networks for building thermal modeling and demand response control

Yongbao Chen^{a,*}, Qiguo Yang^{a,**}, Zhe Chen^a, Chengchu Yan^b, Shu Zeng^c, Mingkun Dai^d

^a School of Energy and Power Engineering, University of Shanghai for Science and Technology, Shanghai, 200093, China

^b College of Urban Construction, Nanjing Tech University, Nanjing, 210009, China

^c College of Foreign Languages, University of Shanghai for Science and Technology, Shanghai, 200093, China

^d School of Mechanical Engineering, Tongji University, Shanghai, 201804, China



ARTICLE INFO

Keywords:

Physics-informed neural networks
Control-oriented modeling
Grid-integrated buildings
Demand response

ABSTRACT

Buildings energy consumption constitutes over 40% of the total primary energy consumption, and buildings can provide potential energy flexibility for the grid. In the grid with high penetration of renewable energy, a control-oriented model with accurate prediction and prompt response is crucial for better load management. However, developing such a model is still a big challenge for grid-integrated buildings due to the limitations of current modeling approaches. Physics-based models commonly represent a specific building while customization for each building remains a daunting task; meanwhile, data-driven models, though easier to develop, require a large amount of data and are not well generalized for other buildings. Thus, we propose a novel model based on a physics-informed neural network dubbed as PhysCon, which combines the interpretable ability of physical laws and the expressive power of neural networks for control-oriented demand response of grid-integrated buildings. Specifically, a Resistance-Capacitance (2R2C) thermal model is adopted to express the knowledge of building physics, and a full-connected neural network is developed to learn the information from actual data. We demonstrate the prediction performance of PhysCon using actual building physics parameters and on-site measured data from an experimental platform that contains two detachable rooms. Two different internal thermal mass scenarios, namely light and heavy mass, were designed to demonstrate the power of PhysCon for buildings with different levels of demand response potentials. The results show that PhysCon outperforms the purely data-driven model in predicting the room temperature and thermal load demand for both light and heavy buildings. Moreover, building thermal mass is an efficient and free demand response resource for grid-integrated buildings. The proposed PhysCon model can be conveniently and efficiently deployed in the energy management system of buildings, owing to its simplicity and generalization.

1. Introduction

1.1. Motivation and related work

Heating, Ventilation and Air Conditioning (HVAC) systems are responsible for 40–60% of the total energy consumption in buildings, and this weather-sensitive energy demand of HVAC systems is the main reason resulting in a relatively short peak load in the power grid, especially in the hottest humid summer days and coldest winter days [1]. This growing peak load demand puts enormous stress on the grid that is under high penetration of intermittent renewable energy (e.g., solar energy and wind power) at present and in the foreseeable future

[2]. Commonly, the peak load demand of the grid lasts for short periods over the year; for instance, the total time of load demand over 90% of the peak load is approximately 100 h, and the total time goes down to 50 h when the load demand is over 95% of the peak load in Shanghai in 2014 [3]. Substantial extra investment is usually required to build standby power plants that are notoriously working with very low efficiency to ensure the grid's stability and safety. To address this problem, Demand Response (DR) has been implemented in the grid-integrated buildings and has been deemed as an important Virtual Power Plant (VPP) for smart grid [4]. In grid-integrated buildings, HVAC systems are the central part of participating DR, owing to the considerable energy flexibility that comes from heat inertia of thermal mass and occupant's

* Corresponding author.

** Corresponding author.

E-mail addresses: chenyongbao@usst.edu.cn (Y. Chen), yangqg@usst.edu.cn (Q. Yang).

behaviors [5,6]. DR program has significant potential to unlock energy flexibility of buildings and to mitigate power imbalance problems caused by the increasing penetration of intermittent renewable energy in the power grid [7]. A widely used strategy in building DR is the global temperature adjustment method for HVAC systems [7,8]. Different percentages of peak load can be reduced or shifted through this method, such as 15–30% reduction lasting for 4–6 h in Ref. [9] and 16–23% reduction lasting for 2 h in Ref. [5].

The building DR control aims for peak load reduction and energy saving as much as possible while maintaining room comfort level within the required range. To do that, a fast, responsive prediction model that accurately represents buildings' thermal dynamics is vitally essential for a building's DR control. Extensive studies have been carried out on the control-oriented thermal modeling of buildings, such as Model Predictive Control (MPC) approach [10,11]. There are typically two models in the MPC approach, including the conventional model based on building physics such as different variants of Resistance-Capacitance (e.g., 2R2C) state space models, and the machine learning models (also data-driven) based on pure historical data such as Artificial Neural Networks (ANN). The related reviews of these two approaches are listed in Table 1.

Grey-box Resistance-Capacitance (RC) model highly relies on the accuracy of the physics-based model. This conventional model requires detailed building physics information and prior knowledge, involving a huge amount of efforts. Viot et al. [24] built an RC thermal model for MPC in an office building to reduce peak load demand and energy consumption. They changed the room temperature setpoint during the unoccupied periods. To improve the reliability of the building model and the performance of building control, the common way is to increase the complexity of the physics-based model or nonlinear solver, which makes it difficult for the conventional RC model to represent a sophisticated energy system, such as a building energy system that is prone to uncertain exogenous conditions. More complicated variants xRyC have been proposed, such as 4R2C [25], 6R4C [26] and 7R3C [27]. Meanwhile, the complexity of the RC model leads to intense computation costs, and the tradeoff between the prediction speed and accuracy should be considered. Zhuang et al. [28] proposed a simplified RC model for MPC in a shopping mall and concluded that an appropriate simplification effectively increases the modeling efficiency and ensures model accuracy simultaneously. Moreover, Zhang et al. [29] used an RC model to evaluate energy flexibility and tested five energy demand flexibility events: real-time pricing, demand limiting, load shedding, load shifting

and load tracking. Although the RC model can realize effective energy saving and better thermal comfort control against the rule-based approach, its initial investment is much higher due to the complex deployment and justification of the MPC system, and thus it is not widely used in commercial applications nowadays [30]. Furthermore, the RC model is heavily dependent on individual buildings and their physics, hence the poor scalable ability of this established model, as discussed in Refs. [31,32].

Due to the aforementioned limitations of conventional RC models, the learning-based MPC approach is rapidly developing owing to its simplicity as well as its utilization of mere building historical data to circumvent the drawbacks of conventional RC models. The widely used learning-based model including conventional machine learning methods such as support vector regression (SVR), XGBoost and random forest (RF), deep learning methods such as long short-term memory (LSTM), artificial neural network (ANN) and convolutional neural networks (CNN) [33,34]. These methods have attracted great scholarly attention due to the fast development of smart buildings that generate massive data throughout their lifetime. For instance, Yang et al. [22] presented a learning-based MPC for real-time building control. Apart from improvement in energy efficiency, indoor thermal comfort was also ameliorated significantly. However, the effectiveness of this model highly depends on the quality and the volume of historical data, resulting in its inapplicability to buildings in the design phase or without enough valuable data. As this model purely relies on historical data, data volume and quality matter a great deal. Data duration of weeks, months, and years was used for developing data-driven models in Ref. [35], and the model's parameters can be continuously involved for better prediction performance owing to the collection and accumulation of new data over time [22]. Apart from the volume of the training dataset, the prediction horizon length is another critical factor that has been investigated, with the computational cost, prediction accuracy and control performance taken into consideration [36,37]. Lee et al. [38] used learning-based MPC to predict indoor temperature and the supply/return water temperature for AC systems in residential buildings, and investigated various prediction horizons. In addition, data augmentation technologies such as autoencoder, generative adversarial networks and transformations are used to increase the model's robustness and prediction accuracies for the case with limited

Table 1
Review of the MPC approach in control-oriented thermal modeling of buildings.

Model types of MPC		Reference	Required inputs ^a	Building types	HVAC system types	Results
RC	4R3C	[12]	IC, ID, ED, SC, EC	Office	TABS	17% energy saving
	Multiple	[13]	IC, ID, ED, SC, EC	Office	FCU	15–20% energy saving
	2R3C	[14]	IC, ID, ED, SC, EC	Office	VAV	5–10% energy cost saving
	Multiple	[15]	EN, IC, ID, ED	Residential	Radiant	64% of thermal discomfort reduction in January and 66% in November
	Low-order	[16]	EN, IC, ID, ED, EC	Lab	Hybrid	31% energy saving
Learning-based	Light-weighted three-phase NNs	[17]	EN, IC, ED, SC	Office	Hybrid	13%–38% energy saving
	Distributed MPC	[18]	EN, IC, ID	Office	Ideal	13% energy saving and 37% thermal comfort improvement
	Multiple Takagi-Sugeno fuzzy model	[19]	EN, IC, ED, SC	Residential	GSHP	62% energy saving and 40% cost saving
	Multiple ANN	[20]	EN, IC, ID, ED	University	TABS	Well represent the most substantial nonlinear effects of building thermal dynamics
	Multiple ANN	[21]	IC, ID, ED, SC	Lab	VRF	30%–70% energy saving
		[22]	EN, IC, ID, ED	Office and Theatre	VAV	59% energy saving in the office and 37% in the theatre

^a Required inputs are divided into six categories based on paper [23]: energy consumption (EN), indoor condition (IC), internal disturbances (ID), external disturbances (ED), system conditions (SC), and envelop conditions (EC).

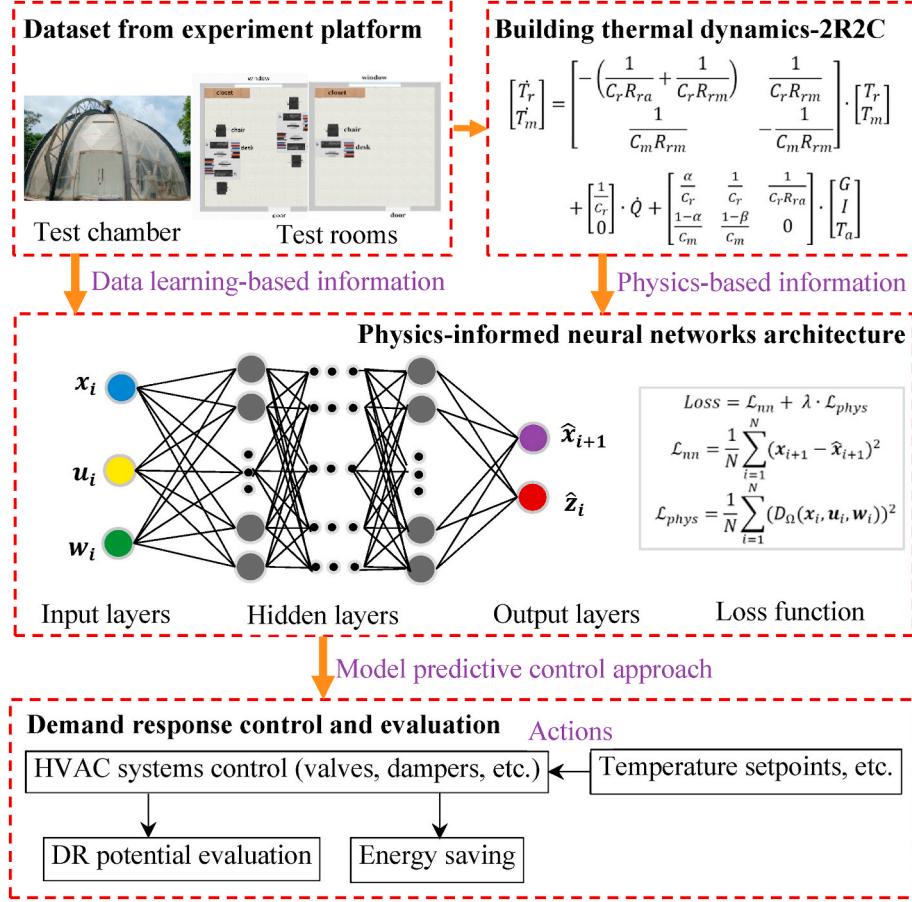


Fig. 1. Workflow of the proposed PhysCon.

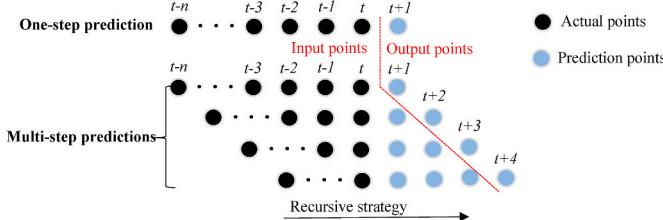


Fig. 2. Concept of one-step and multi-step predictions.

data [39]. Though these learning-based models are easy to develop and convenient to deploy in building control systems, they cannot overcome the drawbacks such as massive data requirement, and lack of interpretability [40] and generalization ability [41]. Hence, despite the promising results, the learning-based model has not yet been widely used in DR control of actual buildings.

The two modeling approaches mentioned above fail to combine the advantages of physics information and real-world data, thus limiting the load management potential of DR in grid-integrated buildings. Therefore, this work aims to bridge the gap between the limitations of conventional physics-based model and purely learning-based approach, by developing a novel model integrating the interpretability of physics-based modeling and the expressive power of learning-based approach, which stands as a promising way to solve control-oriented thermal dynamic problems in DR buildings. Inspired by the Physics-informed Neural Networks (PINNs) in data-driven solution (forward problems) and discovery (inverse problems) of Partial Differential Equations (PDE) in Ref. [42], PINNs have been demonstrated as a compelling architecture that satisfies real-world data and underlying physical laws in

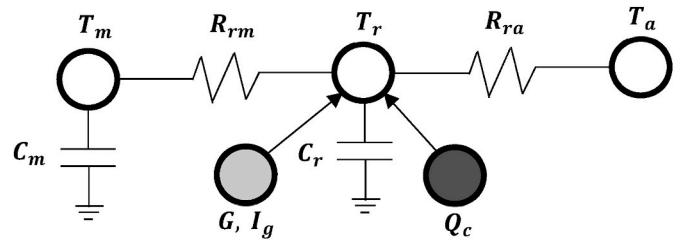


Fig. 3. Illustration of a typical 2R2C model.

various fields, such as fluid thermodynamics, quantum mechanics, and material sciences [43,44]. PINNs have been intruding to model thermal dynamics of buildings in recent years. For instance, Drgona et al. [45] developed a physics-constrained deep learning model for thermal dynamics behavior prediction of buildings; and Gokhale et al. [46] investigated the performance of the PINNs in predicting zone temperature and energy demand. Despite the promising results of PINNs in the thermal dynamics of buildings that have been achieved, few studies have focused on the DR control of grid-integrated buildings. Thus, we present a novel model based on the concept of PINNs, dubbed as PhysCon, for DR control and DR potential evaluation.

1.2. Contributions and novelties

This paper attempts to utilize buildings' physical knowledge and historical data to develop a DR control-oriented model with prompt response and accurate prediction. In this model, PINNs represent the DR control-oriented model of a building's thermal zone, and then this

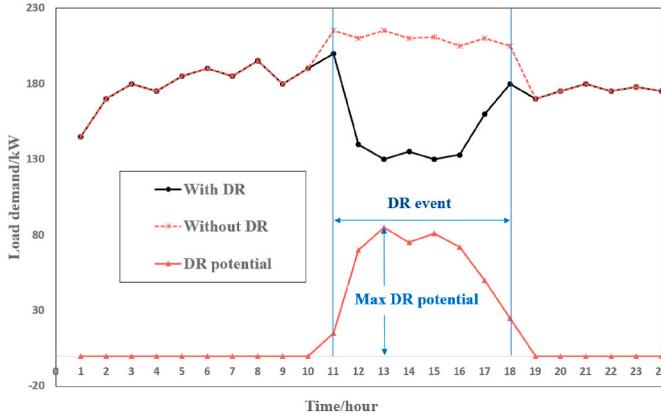


Fig. 4. Illustration of peak load reduction.

validated model is used to evaluate the peak load reduction and energy saving of DR control by changing temperature setpoints. Combining the advantages of the interpretability of building physics and the expressive power of PINNs, we propose a novel DR control-oriented model dubbed PhysCon and demonstrate its effectiveness by designing an experiment with two identical rooms with different amounts of internal thermal mass. Meanwhile, the DR potential of buildings with different amounts and materials of thermal mass is evaluated. The main contributions and novelties of this work are summarized as follows.

- (1) We propose a novel PhysCon model based on PINNs for control-oriented thermal modeling of building DR control. Here, the main thermodynamics parameters of the building are embedded in conventional neural networks, and the results show that the proposed model is robust and scalable. PhysCon achieves higher accuracy in one-step ahead and longer horizon prediction than a pure data-driven model.
- (2) The DR potential (energy flexibility) of different internal thermal mass scenarios is evaluated. Here, heavy and light internal thermal mass rooms are investigated for DR potential evaluation. Owing to the different heat inertia capacities in thermal mass, a ‘heavy’ room provides more DR potential than a ‘light’ room.
- (3) The DR potential of different temperature setpoints is quantified. Here, six setpoint strategies are investigated. In the cooling case, a higher room temperature setting can provide better energy saving while not always bringing higher peak load reduction.

To the author’s best knowledge, this is the first work to combine physics-informed constraints and experimental test data for buildings’ DR control and DR potential evaluation. Compared with traditional pure data-driven models, less historical data size is required in the PhysCon model, which benefits the model users to focus on model exploitation and avoid the expensive and trivial data collection process in practice. In the PhysCon model, real-world data of existing buildings is helpful and other types of physics-based models can replace the RC model. In the future, the PhysCon model can be generalized to different building types and thermal mass scenarios by inputting specific thermophysical parameters, and can be conveniently integrated into the building energy management system to optimize DR. The Python code can be freely downloaded on our GitHub repository and the link is provided at the end of the Conclusion section. The rest of the paper is organized as follows. Section 2 describes the methodology of the proposed PhysCon model. Section 3 establishes an experimental test and describes the data acquisition and processing for PINNs training and testing. Section 4 presents the prediction performance of the PhysCon as well as energy saving and DR potential of different DR controls for heavy and light internal thermal mass scenarios, and the conclusions are drawn in Section 5.

2. Methodology

2.1. Overview of the PhysCon

Given the existing problems in building thermal modeling and DR control as discussed in Section 1, we propose a novel PhysCon model based on PINNs. Fig. 1 gives an overview of the methodology of the PhysCon, which is divided into four sub-sections: 1) acquiring actual data from buildings, 2) building a physics-based thermal dynamics model, 3) training and testing the PINNs, and 4) designing and implementing DR controls and evaluating the DR potential. The detailed information of each part is described as follows. It is worth noting that the real-world data from existing buildings can replace the experimental data and other physics-based models can be used in this model.

2.2. Physics-informed neural networks (PINNs)

Compared with conventional Neural Networks (NNs), we explicitly introduce the physical laws of building thermal dynamics in a fully connected neural network architecture. Then, the PINNs can be trained using measured data. The middle part of Fig. 1 shows the architecture of the PINNs. This network aims to predict the next observation \hat{x}_{i+1} of zone temperature and thermal load demand, and \hat{z}_i of lumped thermal mass temperature, using the current observations as feature inputs that contain current and previous zone temperature x_i , external weather information w_i , energy system’s action u_i and system parameters Ω . D_Ω represents a generic differential operator in the physical section. To embed the physics-based knowledge into a conventional neural network, the loss function is generally reconstructed as in Eq. (1) [46].

$$\text{Loss} = \mathcal{L}_{nn} + \lambda \bullet \mathcal{L}_{phys} \quad (1)$$

$$\mathcal{L}_{nn} = \frac{1}{N} \sum_{i=1}^N (x_{i+1} - \hat{x}_{i+1})^2$$

$$\mathcal{L}_{phys} = \frac{1}{N} \sum_{i=1}^N (D_\Omega(x_i, u_i, w_i))^2$$

where \mathcal{L}_{nn} represents the prediction errors of conventional NNs, and \mathcal{L}_{phys} denotes the physics loss that makes the networks bound to physical laws and prior knowledge. λ is a regularization term that determines the level of physical knowledge usage. In the conventional NNs, λ is set to zero. In the PINNs architecture, two types of predictions can be realized, i.e., one-step ahead prediction of the next state and multi-step predictions of long horizons. Fig. 2 illustrates the concept of these two types of predictions.

2.3. Building thermal dynamics modeling

Resistance-Capacitance (RC) method has been widely used in thermal dynamics modeling, and there are many RC variants with different orders such as 2R2C, 3R2C, and higher order 5R1C [47]. A suitable order of RC is determined by the tradeoff between the complexity and accuracy of modeling. The increase of order brings the improvement of model accuracy, while the model complexity and control response time increase simultaneously. For introducing physical knowledge, we select 2R2C model to follow the physical principle of buildings based on two aspects: 1) 2R2C model was proven to be a simplified and qualified model in building thermal dynamics control [28]; 2) In building DR control, the prompt response of the model is vitally essential. The structure of the 2R2C model is illustrated in Fig. 3, and the state-space equations are defined by Eq. (2).

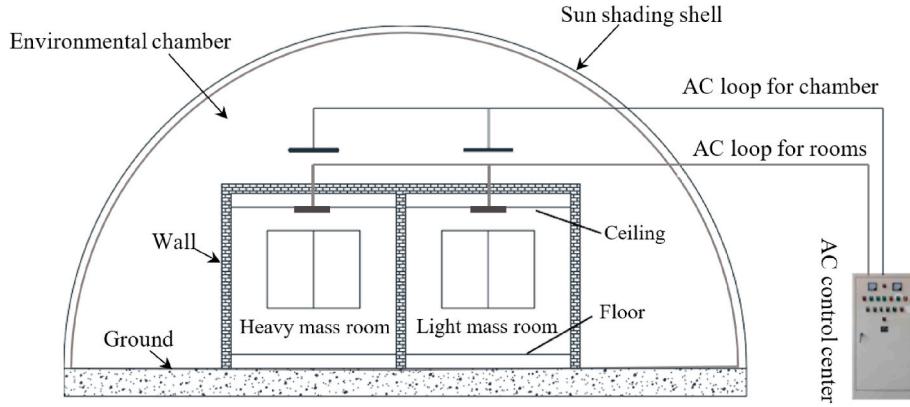


Fig. 5. Schematic of the experiment platform.

$$\begin{bmatrix} \dot{T}_r \\ \dot{T}_m \end{bmatrix} = \begin{bmatrix} -\left(\frac{1}{C_r R_{ra}} + \frac{1}{C_r R_{rm}}\right) & \frac{1}{C_r R_{rm}} \\ \frac{1}{C_m R_{rm}} & -\frac{1}{C_m R_{rm}} \end{bmatrix} \bullet \begin{bmatrix} T_r \\ T_m \end{bmatrix} + \begin{bmatrix} \frac{1}{C_r} \\ 0 \end{bmatrix} \bullet \dot{Q} \\ + \begin{bmatrix} \frac{\alpha}{C_r} & \frac{1}{C_r} & \frac{1}{C_r R_{ra}} \\ \frac{1-\alpha}{C_m} & \frac{1-\beta}{C_m} & 0 \end{bmatrix} \bullet \begin{bmatrix} G \\ I \\ T_a \end{bmatrix} \quad (2)$$

where \dot{T}_r is the room temperature of the next state, and \dot{T}_m is the building's lumped thermal mass temperature of the next state; T_r , T_m , and T_a are the current temperature of the room, lumped thermal mass, and ambient, respectively; C_r and C_m are the thermal capacitances of room air and lumped thermal mass; R_{ra} is the thermal resistances between the room and outside air, and R_{rm} is the thermal resistances between the room and thermal mass; G and I are the solar irradiances and internal heat gains, and α is the solar irradiance absorption factor. \dot{Q} represents the thermal load supply from the AC, which can be defined by Eq. (3).

$$\dot{Q} = \dot{m}c_p\Delta T = \dot{m}c_p(T_s - T_r) \quad (3)$$

where \dot{m} and T_s are the mass air flow rate and temperature of supply air, respectively; c_p is the specific heat capacity of air. The thermal load supply can be determined by changing the AC system's actions, such as

the opening control of the valves and dampers, i.e., $\dot{Q} = f(u)$. Here, it is ON when $f(u) < 0$ in the cooling supply case, and vice versa.

Physical knowledge can be introduced through continuous time state-space equations in Eq. (2) that are rewritten to discrete-time Eq. (4), using a first-order Euler discretization method.

$$\begin{bmatrix} T_{r,i+1} \\ T_{m,i+1} \end{bmatrix} = a \bullet \begin{bmatrix} T_{r,i} \\ T_{m,i} \end{bmatrix} + b \bullet \dot{Q}_i + c \bullet \begin{bmatrix} G_i \\ I_i \\ T_{a,i} \end{bmatrix} \quad (4)$$

$$= \begin{bmatrix} -a_{11} & a_{12} \\ a_{21} & -a_{22} \end{bmatrix} \bullet \begin{bmatrix} T_{r,i} \\ T_{m,i} \end{bmatrix} + \begin{bmatrix} b_1 \\ 0 \end{bmatrix} \bullet \dot{Q}_i + \begin{bmatrix} c_{11} & c_{12} & c_{13} \\ c_{21} & c_{22} & 0 \end{bmatrix} \bullet \begin{bmatrix} G_i \\ I_i \\ T_{a,i} \end{bmatrix} \quad (4)$$

where parameters a , b , c represent the physical knowledge of the building, which can be calculated based on real building measurements

Table 2
Thermal mass category of heavy and light mass scenarios.

Scenarios No.	Internal mass category
Scenario 1 (light mass)	Office desk and chair: 1 set, 60 kg Files and closet: 75 kg Others: 50 kg
Scenario 2 (heavy mass)	Office desk and chair: 4 sets, 240 kg Files and closet: 300 kg Others: 200 kg

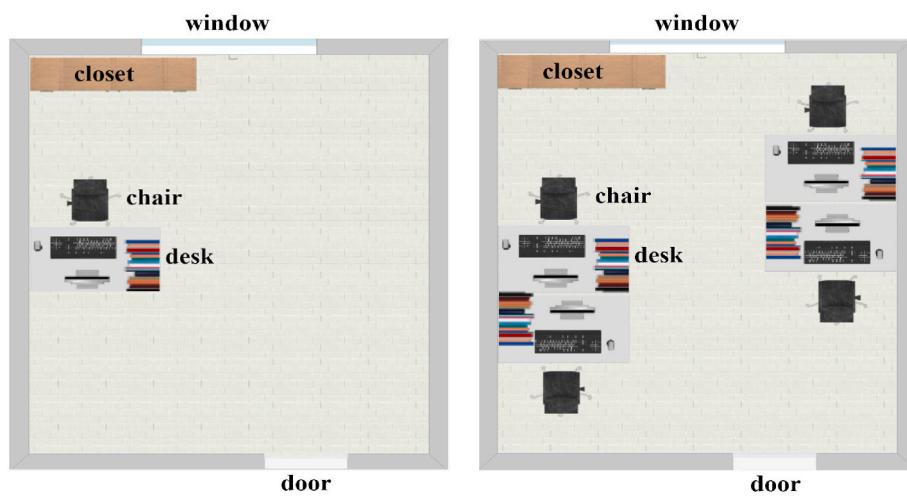


Fig. 6. Layout of different internal thermal mass scenarios.

Table 3

Detailed information of envelope and internal thermal mass of the rooms.

Components	Types	Geometric parameters			Thermophysical parameters		
		Area m ²	Thickness m	Materials	Density Kg/m ³	Conductivity W/(m·K)	Specific heat kJ/(kg·K)
East wall	External wall	14.94	0.17	Plate + Insulation board	150	0.045	1.22
West wall	Partition wall	14.94	0.17	Plate + Insulation board	150	0.045	1.22
South wall	External wall	7.07	0.17	Plate + Insulation board	150	0.045	1.22
North wall	External wall	8.58	0.17	Plate + Insulation board	150	0.045	1.22
South window	External window	3.40	—	Glass	2500	0.043	0.84
North door	External door	1.89	—	Glass	2500	0.043	0.92
Ceiling	Suspend	14.89	—	Gypsum board	1050	0.330	2.01
Ground floor	Suspend	14.89	0.04	Silicate board	7850	58.20	0.48
Furniture	Internal mass	—	0.02–0.03	Plywood + Paper	600	0.170	2.51

Table 4Calculation results of parameters a , b , c in Eq. (4).

Scenarios No.	a	b	c
Scenario 1 (Light mass)	$a_{11} = 2.26 \times 10^{-3}$	$b_1 = 1.20 \times 10^{-5}$	$c_{11} = 1.20 \times 10^{-5}$
	$a_{12} = 1.99 \times 10^{-3}$		$c_{12} = 1.20 \times 10^{-5}$
	$a_{21} = 3.62 \times 10^{-5}$		$c_{13} = 1.20 \times 10^{-5}$
	$a_{22} = 3.62 \times 10^{-5}$		$c_{21} = 2.69 \times 10^{-4}$
			$c_{22} = 0$
Scenario 2 (Heavy mass)	$a_{11} = 1.49 \times 10^{-3}$	$b_1 = 1.20 \times 10^{-5}$	$c_{11} = 1.20 \times 10^{-5}$
	$a_{12} = 1.22 \times 10^{-3}$		$c_{12} = 1.20 \times 10^{-5}$
	$a_{21} = 3.75 \times 10^{-5}$		$c_{13} = 1.20 \times 10^{-5}$
	$a_{22} = 3.75 \times 10^{-5}$		$c_{21} = 2.69 \times 10^{-4}$
			$c_{22} = 0$

or estimated based on a pure data-driven model. For the estimation case, these parameters can be initialized to a specific value and then tuned during the training process using on-site data. Therefore, this model could work regardless of the provision of thermodynamics parameters. Given this 2R2C model, the loss function in Eq. (1) can be rewritten as follow.

$$\begin{aligned}\mathcal{L}_{nn} &= \frac{1}{N} \sum_{i=1}^N (T_{r,i} - \hat{T}_{r,i})^2 + \frac{1}{N} \sum_{i=1}^N (u_{r,i} - \hat{u}_{r,i})^2 \\ \mathcal{L}_{phys} &= \frac{1}{N} \sum_{i=1}^N (T_{m,i} - \hat{T}_{m,i})^2\end{aligned}\quad (5)$$

Using a 2R2C structure, the thermal mass temperature (T_m) can be computed, as shown in Eq. (6).

$$T_{m,i} = \frac{1}{a_{12}} (\dot{T}_{r,i} + a_{11} \hat{T}_{r,i} - b_1 \dot{Q}_i - c_{11} G_i - c_{12} I_i - c_{13} T_{a,i}) \quad (6)$$

$$\dot{T}_{r,i} = \frac{T_{r,i+1} - T_{r,i}}{\Delta t}$$

where $\hat{T}_{r,i}$ is the room temperature of the state i and $T_{m,i}$ is lumped thermal mass temperature of the state i that can be calculated using Eq. (6). In this way, the loss function in Eq. (5) is bound to physical laws.

2.4. Demand response potential evaluation

DR potential (also energy flexibility ability) denotes the ability of peak load reduction or valley load increment in DR events, as shown in Fig. 4. The DR potential of buildings is vital for the power grid with high penetration of renewable energy to balance the power supply and demand. The grid-integrated building is a building with high energy

flexibility and an advanced energy management system to optimize energy use and provide grid services. The DR potential DR_p can be defined as Eq. (7).

$$DR_p = (P_{DR} - P_{baseline}) / Area \quad (7)$$

where P_{DR} is the peak load demand in the DR control case, $P_{baseline}$ is the peak load demand without DR control, and $Area$ is the total building area.

Within a wide comfort range (such as ± 2 °C of room temperature) of the thermal zone, the HVAC systems usually have considerable energy flexibility that can be utilized by resetting zone temperature and controlling water and air flow rate [7]. Conventionally, physics-based tools such as EnergyPlus, TRNSYS, and Modelica, are widely used to estimate the energy flexibility of buildings [34]. However, these tools have been designed to solve ordinary differential equations along with much detailed physics information and prior knowledge that are difficult to obtain; thus, they are unsuitable for DR control in buildings. In this paper, the proposed PhysCon model incorporating the 2R2C model and PINNs architecture is feasible for MPC in DR building energy management systems. Thermal load supply (action u) is one of the inputs in the PINNs architecture, and this action changes for the next states according to the difference between the predicted room temperature (\hat{x}_{i+1}) and the temperature setpoint so that the real thermal load demand can be estimated.

The DR_p of HVAC system highly depends on the temperature resetting that deviates from the regular setting. To evaluate the DR potential of HVAC systems by different temperature setpoints in the whole DR event, Eq. (7) can be rewritten to Eq. (8).

$$DR_p = \max ((P_{DR,\Delta T_i} - P_{baseline}) / Area) \quad (8)$$

where ΔT_i is the resetting temperature deviation from the regular set at time step i . To avoid the occurrence of a second peak load after a DR event, three different linear temperature resetting approaches, including “Slow Rise”, “Fast Rise” and “Maximum Rise”, have been introduced in Ref. [48].

3. Data acquisition and model development description

3.1. Experiment platform

The schematic of the experiment platform is shown in Fig. 5. Two testing rooms with an area of 16 m² for each are inside the controllable environment chamber. In Fig. 5, the left room (the eastern one) was designed to represent a heavy internal thermal mass layout, and the right room (the western one) represents the case of light internal mass. The heavy mass layout represents a heavy occupancy working scenario (four people), and the light mass one is a light occupancy (private office). The temperature and humidity of the chamber and the rooms were controlled using two independent air-water AC. Solenoid valves with proportion-integration-differentiation controllers were installed into the AC loop to respond to thermal load demand. The air volume of the fan coils was manually divided into three levels: high, medium, and low.

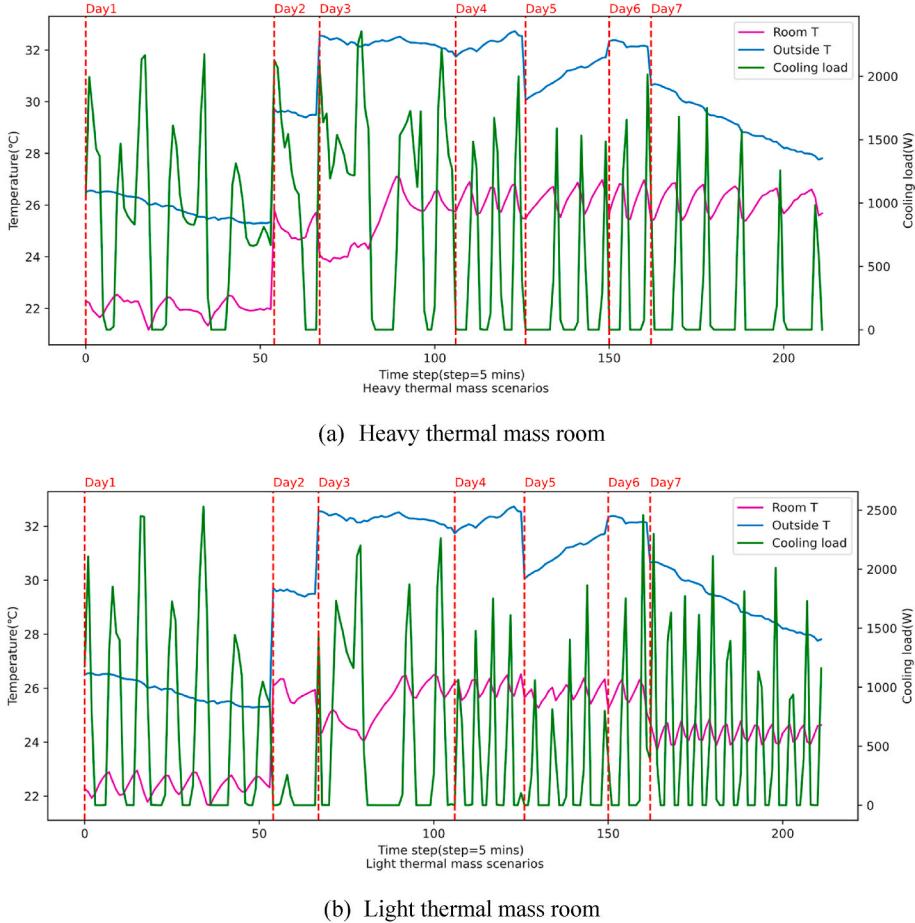


Fig. 7. Training data profiles for the PINNs architecture.

Table 5
Hyperparameters for the PhysCon model.

Parameters	Value setting
Activation function	tanh
Learning rate	0.001
Hidden layers	2
Neurons per layer	64
Optimizer	Adam
Batch size	30

Under this circumstance, the temperature control accuracy of the rooms and the chamber was ± 0.5 °C. The room temperature setpoints were manually configured on the panels of the AC control center. We set the

room temperature to 22 °C, 24 °C, and 26 °C to test the thermal dynamics characteristics of the room, respectively, which simulates the common zone temperature resetting strategies in DR event [3]. To validate our proposed PhysCon and investigate the effects of internal thermal mass on DR potential, two scenarios of heavy and light thermal mass were established, as illustrated in Fig. 6. Table 2 presents detailed information of the building thermal mass. For practical purposes, the heavy scenario usually represents the heavy occupancy office room, and the light one is for the light occupancy room. More detailed information of the experiment platform can be found in our previous works [49].

The detailed thermophysical parameters listed in Table 3 were used to calculate the parameters a , b , c in Eq. (4), and the results for these two scenarios are listed in Table 4. It is worth noting that the thermal capacitances, resistances, and area are specified and can usually be measured in the case of experimental study; thus, we provide the specific

Table 6
MAEs and CVRMSE of different regulation terms λ .

Regulation term λ	MAE of temperature in heavy scenario (°C)	CVRMSE of temperature in heavy scenario	MAE of load in heavy scenario (W)	CVRMSE of load in heavy scenario	MAE of temperature in light scenario (°C)	MAE of load in light scenario (W)
0.0	0.4709	2.2%	123.31	18.3%	0.4049	220.12
0.1	0.2408	1.1%	102.70	16.3%	0.2169	286.46
0.2	0.2436	1.1%	104.67	16.4%	0.2233	315.55
0.3	0.2441	1.1%	106.55	16.6%	0.2438	330.95
0.4	0.2483	1.1%	108.39	16.8%	0.2422	346.26
0.5	0.2547	1.2%	110.15	17.1%	0.2480	349.79
0.6	0.3976	1.8%	127.23	20.6%	0.2748	349.21
0.7	0.4335	1.9%	132.33	21.6%	0.2793	353.09
0.8	0.4483	2.0%	134.75	21.9%	0.2770	356.26
0.9	0.4621	2.0%	137.59	22.3%	0.2722	361.53
1.0	0.4746	2.1%	141.35	22.7%	0.2652	366.08

Table 7MAEs and CVRMSE of different selections of Time-lag t_l .

Time-lag t_l (5 min each lag)	MAE of temperature in heavy scenario ($^{\circ}$ C)	CVRMSE of temperature in heavy scenario	MAE of load in heavy scenario (W)	CVRMSE of load in heavy scenario	MAE of temperature in light scenario ($^{\circ}$ C)	MAE of load in light scenario (W)
0	0.3984	1.9%	130.77	20.8%	0.4560	298.34
1	0.2547	1.2%	110.15	17.1%	0.2480	349.79
2	0.2851	1.3%	110.35	17.6%	0.2002	336.75
4	0.6594	3.0%	141.34	22.0%	0.2170	222.50
6	0.3648	1.7%	120.18	18.9%	0.1728	363.44
8	0.5252	2.6%	151.93	23.6%	0.6756	347.64
10	0.4699	2.2%	169.94	25.3%	0.4760	332.58

a, *b*, *c* directly. However, given the difficulties in acquiring the thermophysical parameters of most existing buildings, they can be estimated by developing NNs or other data-driven models using the same historical data. Apart from the thermophysical parameters of building physics, as

shown in Eq. (4), heat gains, including solar gain (G) and other internal heat gains (I), are required. We set $G = 0$ because we closed the sun shading shell during the test and set $I = 16 * 11 \text{ W}$ for both testing rooms. For different building types and thermal mass scenarios, the

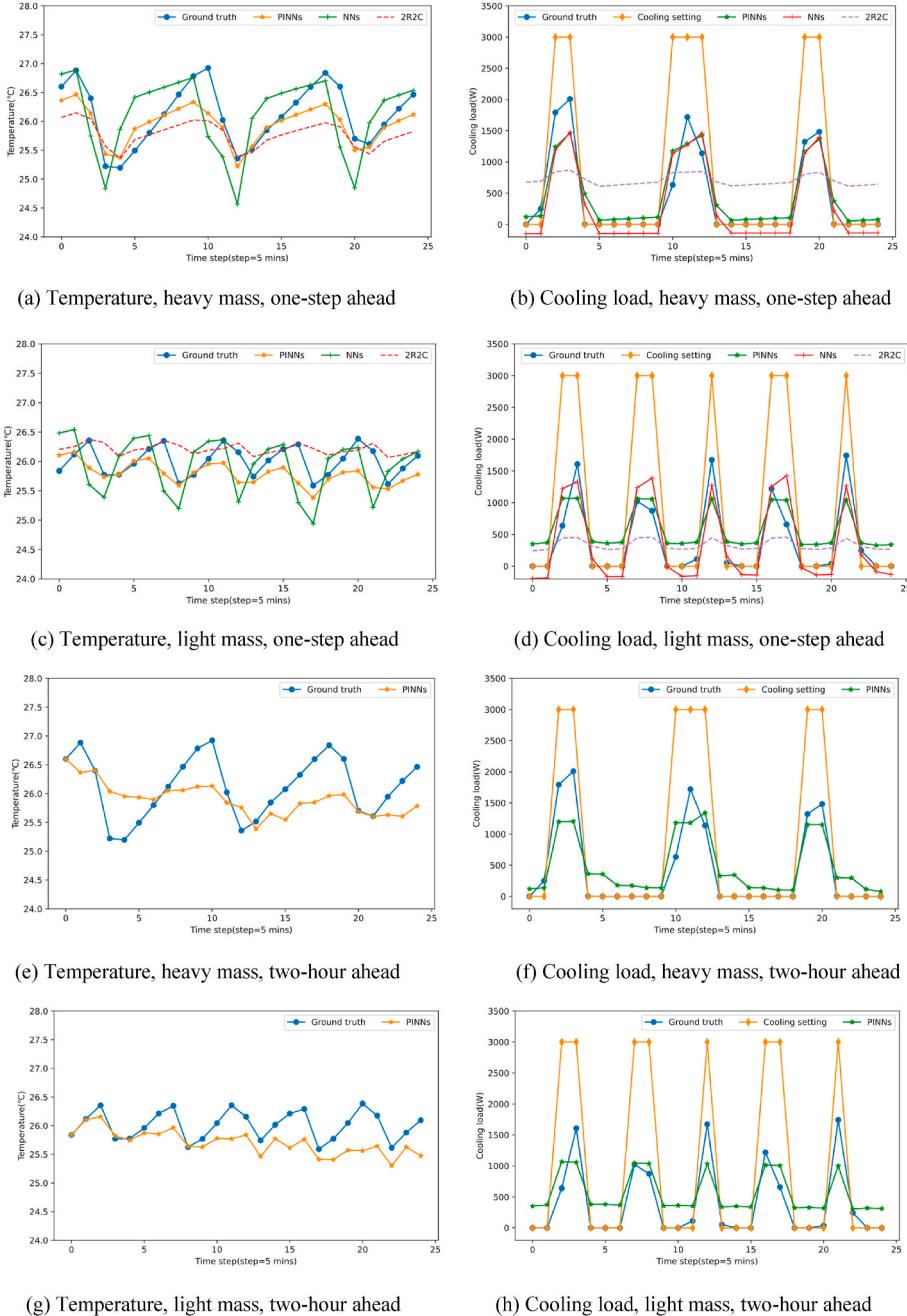
**Fig. 8.** Prediction results comparison of one-step ahead (i.e., 5 min ahead) and long horizons (i.e., 2-h ahead) in heavy and light mass scenarios.

Table 8

MAEs and CVRMSE comparison of PINNs and NNs model in different scenarios.

		PINNs-heavy mass	PINNs-light mass	NNs-heavy mass	NNs-light mass
MAEs	Temperature (°C)	0.25	0.24	0.47	0.40
	Cooling load (W)	110.15	142.03	194.79	202.92
CVRMSE	Temperature	1.2%	1.2%	2.2%	1.9%
	Cooling load	17.1%	22.8%	29.7%	31.3%

proposed model can be trained by using different thermophysical parameters shown in Table 4 and can be conveniently and efficiently deployed in building control systems.

3.2. Data acquisition description

The real-time temperature and cooling load supply of AC were measured employing ADAM-4118 modules, which were connected to the computer data acquisition application through an RS-485 serial port. T-type thermocouple thermometer (with the temperature measurement range of $-200\text{--}350\text{ }^{\circ}\text{C}$ and the measuring accuracy of $\pm 0.1\text{ }^{\circ}\text{C}$) and calorimeter Shark-773 were used to measure temperature and cooling load, respectively. To simulate a regular DR event, we opened AC systems in the early morning to keep the temperature of internal thermal mass close to room air temperature to avoid the effect of the initial temperature of the building thermal mass, and we implemented DR events and acquired valid data in the afternoon. Data of seven days were measured for training, and an extra day was adopted for model testing. It should be noted that the measured time horizons (from 1 to 5 h) were not the same for each day, so regular DR event durations were covered in practice.

3.3. Model development process

Training data size determines the performance in learning-based models. However, the data availability of buildings has no guarantee in practice. Using less data size to develop a good generalization and robustness model is pretty promising. This paper aims to use limited data to develop a robustness model utilizing physical knowledge simultaneously. Specifically, a data size (236 samples for each thermal mass scenario) of eight days was used to train and test our model. The dataset of seven days (212 samples for both) was adopted as the training dataset, and that of the remaining day (24 samples for both) was the testing dataset. The training dataset of the heavy and light mass rooms can be seen in Fig. 7, and the measured granularity was averaged to 5 min (i.e., the time step of the model). To simulate the temperature resetting strategies in the DR event, three common settings $22\text{ }^{\circ}\text{C}$, $24\text{ }^{\circ}\text{C}$, and $26\text{ }^{\circ}\text{C}$ were set for both rooms during the experiment test. Furthermore, to investigate the real DR events, a duration of one to 5 h was scheduled during the training data acquisition process. The testing data can be found in section 4. On these experiment days, external temperature, namely chamber temperature, varied from $25.2\text{ }^{\circ}\text{C}$ to $32.7\text{ }^{\circ}\text{C}$, and room temperature ranged from $21.1\text{ }^{\circ}\text{C}$ to $27.2\text{ }^{\circ}\text{C}$.

Once the data was split for the training process, we set the regulation term λ to 0.5 to search for the best value setting of hyperparameters, and Table 5 presents the hyperparameters chosen in the model. Pytorch Lightning package (version 1.6.3) was used to implement the PhysCon model, and we run our code on the Jupyter lab web platform.

4. Results and discussions

We first search for the best regulation term (λ) and time-lag (t_l) and then present the results and the DR potential of the PhysCon. Two thermal mass scenarios of office building style were considered for

testing our proposed PhysCon model and evaluating the DR potential by changing temperature setpoints.

4.1. Regulation term λ and time-lag t_l

In our proposed PhysCon model, the current states of room temperature (x_i), outside air temperature (w_i), AC system's action (u_i), and thermal load demand (x_i) were used to determine the subsequent observations of room temperature and thermal load demand (\hat{x}_{i+1}). The amount of past information used in PhysCon matters, including previous states of room temperature and thermal load, is conducive to increasing prediction accuracy [50]. Thus, different sizes of previous states called time-lags (t_l) were investigated. Additionally, since the amount of physical knowledge that should be incorporated in the PhysCon model is crucially important, the regulation term λ is adopted to represent how much physics knowledge is associated with neural networks. A good model appropriately takes into consideration both real-world conditions (on-site data) and underlying laws (conservation equations), and thus we ran $\lambda = 0.1, 0.2, \dots, 1.0$ to search for the best selection. Table 6 presents the results of using different λ ranging from 0.0 to 1.0. We found that the results of λ ranging from 0.1 to 0.5 are very close. Introducing more physical information into the PhysCon model would make the model more robust to our intuition. Thus, where $\lambda = 0.5$ is chosen as the optimal value that helps achieve a room temperature Mean Absolute Error (MAE) of $0.25\text{ }^{\circ}\text{C}$ and Coefficient of the Variation of the Root Mean Square Error (CVRMSE) of 1.2%. To tune for the best time-lags (5 min for each lag), $t_l = 0, 1, 2, \dots, 10$ were investigated based on the optimal $\lambda = 0.5$ and $t_l = 1$ is found to yield the best prediction results, as shown in Table 7. The optimal selection of these two parameters contributes to a better estimation of room temperature and thermal load demand. Therefore, this selection approach and the recommended values of λ and t_l could be a reference for buildings of the same type.

4.2. Prediction results

Two scenarios, including heavy and light internal thermal mass, were designed to test the PhysCon. The objective of these experiments is twofold: 1) to test the PINNs architecture in predicting zone temperature and thermal load demand; 2) to test the PhysCon as a control-oriented predictive model to investigate the DR potential of buildings. In our experiments, the dataset of seven days was adopted as the training dataset, and that of the remaining day was the testing dataset. We aim to test the advantages of introducing more underlying physics knowledge, so two prediction architectures, i.e., PINNs and NNs, were developed to do that.

DR events usually last for a short time (e.g., 1–2 h) when the grid is under high pressure in extreme weather or in emergencies. Thus, a span of 2 h was investigated in this paper. Fig. 8 (a) – (d) display the prediction results of PINNs and NNs, and the cooling setting is the designed cooling load demand. For both heavy and light thermal mass scenarios, the room temperature prediction results follow the ground truth closely, which attests to the good prediction performance of the PINNs. Table 8 presents the MAEs and CVRMSE of room temperature in degrees Celsius and cooling load demand in Watts, with conventional NNs used as the benchmark. For the heavy mass scenario, the PINNs obtain a MAE of $0.25\text{ }^{\circ}\text{C}$, which outperforms $0.47\text{ }^{\circ}\text{C}$ of NNs, and this advantage can also be seen in the light mass case. The cooling load demand results suggest close MAE for both networks. The results prove that the proposed PhysCon can reasonably estimate the thermal dynamic of buildings and thus would be a promising modeling approach for DR control.

Apart from predicting the one-step ahead (5 min ahead) state, the long horizons state can be realized through a recursive strategy. One-step ahead prediction uses the actual values as inputs to estimate the next state, which is beneficial to energy and operational cost saving, while multi-step prediction presents an array of outputs for long horizons, such as days and months ahead, which is helpful to future energy

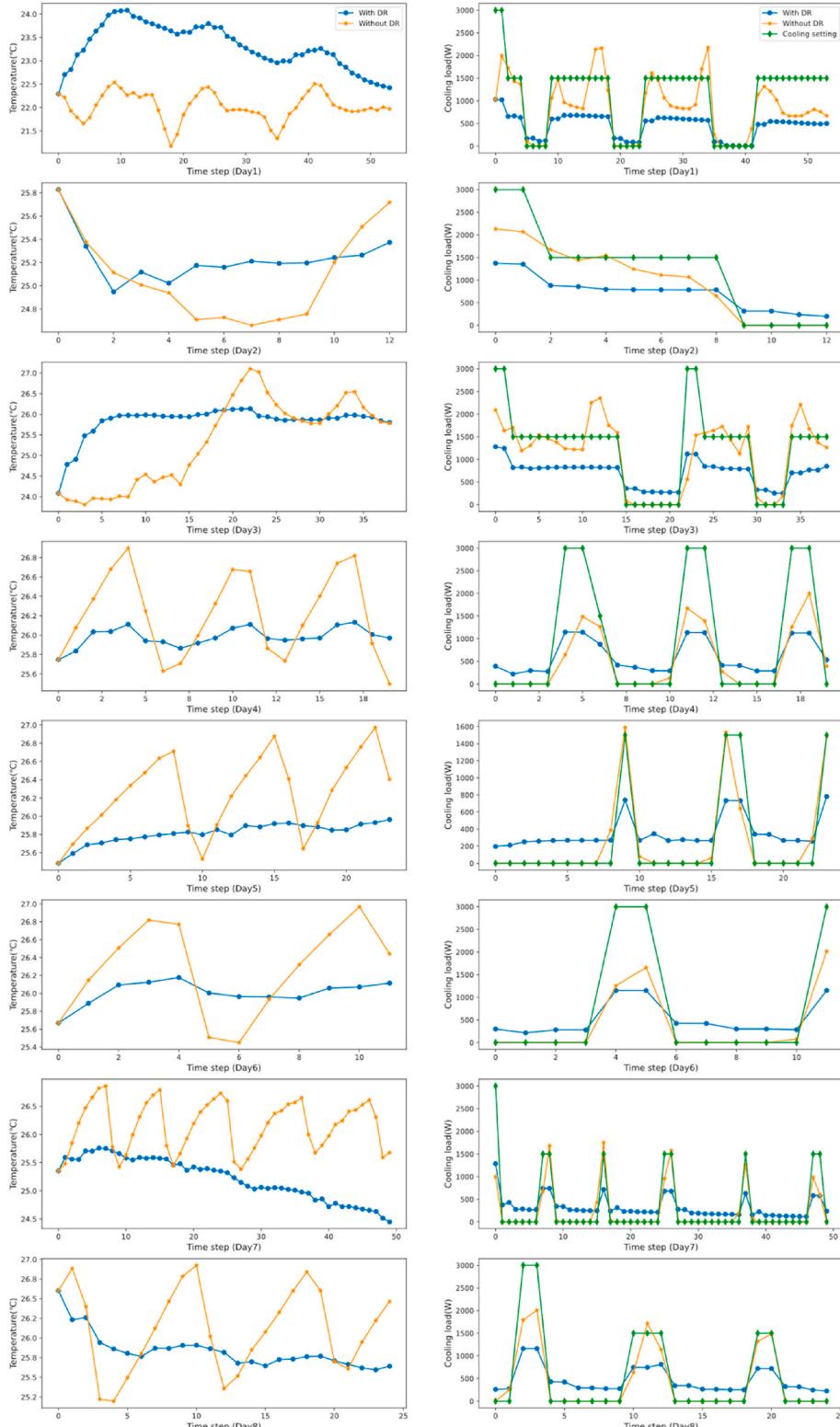


Fig. 9. DR potential results of heavy mass room (room temperature set from 24 °C to 26 °C).

planning and management. As illustrated in Fig. 2, the outputs were fed back as inputs to the networks to yield multi-step predictions of the long horizons state. However, errors would accumulate for each iteration and further lead to a more significant bias in the end. We tested the long horizons of 24 steps ahead (2-h ahead) using the recursive approach mentioned in section 2.2, and as the results in Fig. 8 (e)–(f) have shown, the predictions are not as good as the one-step ahead prediction, while

the MAE of temperature is still lower than 0.5 °C (0.41 °C and 0.31 °C for heavy and light mass respectively).

The zone temperature continuously changes within the comfort range during DR events, making it difficult to achieve accurate prediction through conventional data-driven approaches, such as long short-term memory and convolutional neural network [51]. In one-step ahead prediction, the PINNs could follow the ground truth closely

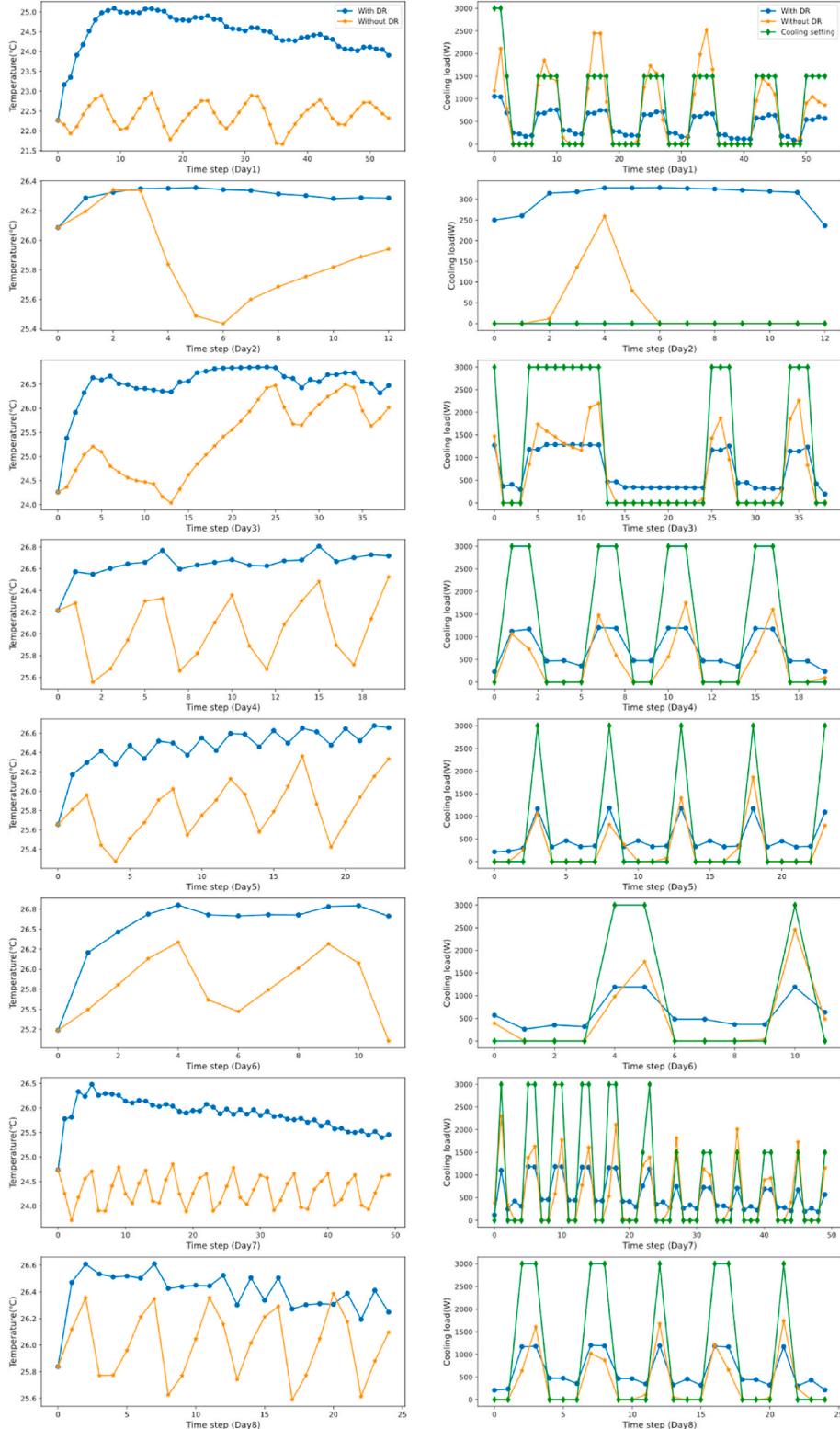


Fig. 10. DR potential results of light mass room (room temperature set from 24 °C to 26 °C).

despite the constantly fluctuating temperature and cooling demand in both thermal mass scenarios. This proves that a physics-informed approach is promising for MPC building DR.

4.3. DR potential

The proposed PhysCon model can help estimate the thermal load

demand by changing the room temperature setting. Generally, the comfort temperature of buildings has a wide range, such as from 24 °C to 26 °C for office buildings according to Chinese standards [52]. Conventional RC models have been in extensive use for MPC in buildings, but they require significant modeling efforts to achieve satisfactory prediction accuracy [31]. With its advantages of better generalization and faster computational ability, the PhysCon model has the potential to

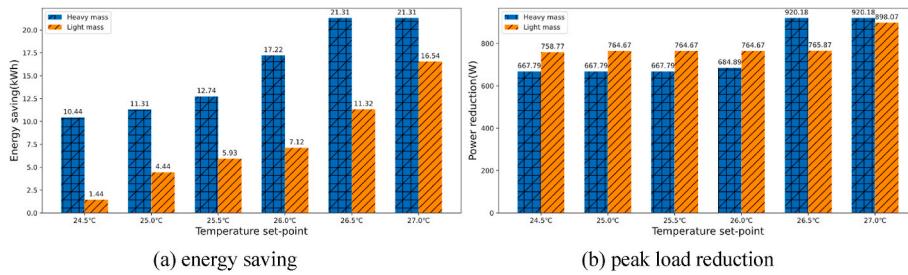


Fig. 11. Energy saving and power reduction results using the temperature resetting approach (The load reduction equals the peak load without DR control deducting the peak load with DR control during the whole DR event, which can be seen in Eq. (8)).

be applied in the DR field.

The room temperature was set at 24 °C as the benchmark to evaluate the DR potential. The end-users' requirements and behaviors are affected by age, gender, economic incentives and various other factors, and thus zone temperatures slightly out of the comfort range generally would not bring forth complaints or rejections, which means a broader temperature range could afford more energy flexibility. In incentive DR programs, the customers are willing to set the room temperature over the upper limit (i.e., up to 27 °C) in order to gain extra rewards [5]. Hence, we set six different resetting strategies, including 24.5 °C, 25.0 °C, 25.5 °C, 26.0 °C, 26.5 °C and 27.0 °C for eight days, respectively. Figs. 9 and 10 show the results of the 26 °C setpoint for heavy and light mass scenarios. The other setpoint results can be seen in Appendix Figure A, and the high-quality figures of each setpoint can be found in our open-access Jupyter notebook, the link of which is listed below. The blue circle curves illustrate the case with DR control, and the yellow star curves present the cases without DR control.

Peak load reduction or shifting constitutes the primary goal to ensure grid safety in buildings; meanwhile, the owner could be penalized if the actual peak load demand exceeds the initially purchased quota [53,54]. Fig. 11 shows the total average energy saving and peak power reduction of all days. It can be seen that energy saving improves as a higher temperature is set, which is compatible with our expectations. Moreover, compared with the light mass case, energy saving is prominently higher in the heavy mass scenario, which is consistent with our intuition that the internal thermal mass has the function of thermal storage. It is worth noting that internal heat gain remains the same for both scenarios in our experiment while it could be different in practice. However, power reduction is approximate in both scenarios. For setpoints of 24.5 °C, 25.0 °C, 25.5 °C, and 26.0 °C, the power reduction of heavy mass is lower than that in the light mass case.

As shown in Fig. 9 and Appendix Fig. A, the peak load usually lasts for a short time, which is the leading cause for high pressure in the grid. In Fig. 11, we found that energy saving ability does not mean a correspondent capability of peak load reduction. In the cooling season, increasing the temperature setpoint could apparently contribute to energy saving, while peak load reduction is not as good as energy saving. A bigger temperature setpoint difference in each step is required to obtain a higher peak load reduction, which runs the risk of discomfort for end-users. In a heavy thermal mass scenario, heat inertia of thermal mass functions as passive energy storage materials that could mitigate the risk of discomfort, despite a larger setpoint difference. In this paper, we adopt the same setpoint strategies for both thermal mass scenarios, although different setpoint strategies for different mass scenarios could be an interesting foci for future research. Moreover, pre-cooling, widely applied in building DR, could increase the DR potential efficiently even though more energy is usually consumed.

5. Conclusions

This paper proposes a novel PhysCon model based on physics-informed neural networks (PINNs) for demand response (DR) control

in grid-integrated buildings. A 2R2C thermal model and conventional full-connected neural networks (NNs) are associated with the PhysCon model. The prediction results show that the PhysCon model performs well for predicting the room temperature and thermal load demand, with a lower MAE of 0.25 °C and CVRMSE of 1.2% of room temperature and MAE of 110 W and CVRMSE of 17.1% of cooling load demand in the heavy thermal mass scenario, compared with the MAE results of 0.47 °C (CVRMSE of 2.2%) and 195 W (CVRMSE of 29.7%) of the conventional neural network. For the light thermal mass scenario, the PINNs architecture also achieves lower prediction errors. This indicates that the PhysCon model is adequate for thermal modeling in grid-integrated buildings.

Moreover, using PhysCon for model predictive control, we investigate the DR potential by changing temperature setpoints. The results show that energy saving potential strongly and positively correlates with temperature setpoints, while peak load reduction potential does not show similar correlations. A proper temperature setpoints strategy is beneficial to increasing peak load reduction for buildings with different amounts and materials of thermal mass. In the PhysCon model, the physical parameters in PINNs structure can be calculated using actual building physics information or estimated using the same developed NNs. Owing to these merits, this proposed PhysCon model is easily scalable and deployable. The main conclusions are summarized as follows.

- (1) Compared with pure data-driven model neural networks (NNs) and physic-based grey-box model 2R2C, the PhysCon model performs better in predicting thermal dynamics states with a lower prediction error of temperature (MAE is less than 0.25 °C); besides, less amount of data size is required in the PhysCon model.
- (2) How much physical knowledge incorporating into the PhysCon matters. The amount of physical knowledge regulation term λ ranging from 0.1 to 0.5 is the optimal value for an office building scenario.
- (3) Compared with active approaches such as the installation of energy storage devices, the zone temperature setting is a cost-efficient passive approach to provide energy flexibility in buildings without sacrificing the occupants' comfort much. Approximately 40% of peak load reduction can be achieved by setting a zone temperature 2 °C higher in the cooling case.

Future work could focus on: (a) prediction performance of different variants of RC and NNs structures; (b) pre-cooling strategy in improving peak load reduction potential; (c) deployment of the proposed PhysCon model in building cluster and city-size DR programs.

For the detailed information regarding the code, please refer to our GitHub reservoir on: <https://github.com/Bob05757/PINNs-for-building-thermal-modeling-and-Demand-Response>.

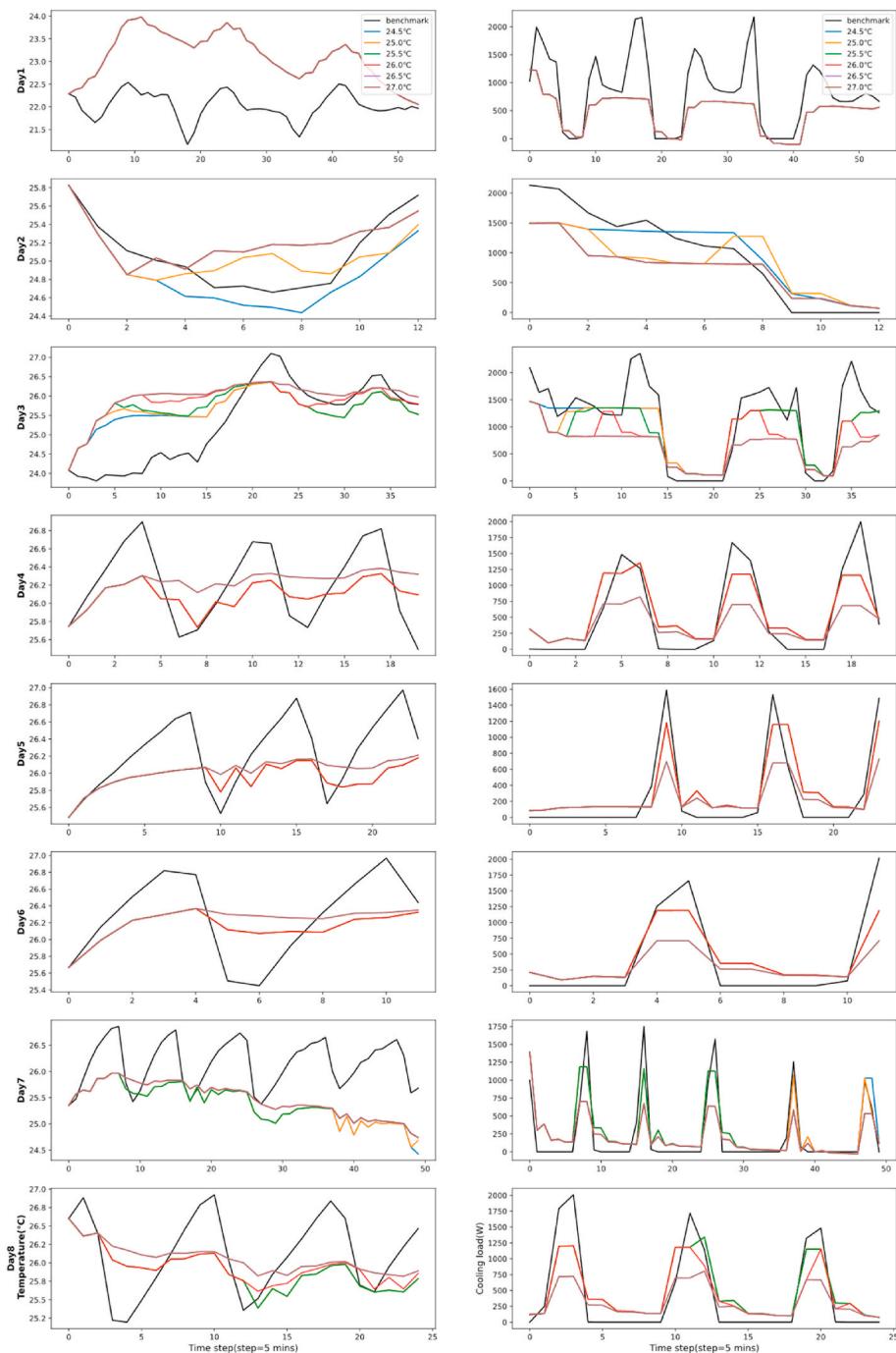


Fig. A. Temperature and cooling load demand results of different temperature setpoints, including 24.0 °C (benchmark), 24.5 °C, 25.0 °C, 25.5 °C, 26.0 °C, 26.5 °C, 27.0 °C

CRediT authorship contribution statement

Yongbao Chen: Writing – original draft, Methodology, Funding acquisition, Formal analysis, Conceptualization. **Qiguo Yang:** Methodology, Conceptualization. **Zhe Chen:** Software. **Chengchu Yan:** Investigation. **Shu Zeng:** Writing – review & editing. **Mingkun Dai:** Writing – review & editing.

Declaration of competing interest

The authors declare that they have no known competing financial interests or personal relationships that could have appeared to influence the work reported in this paper.

Data availability

I have shared the data and code links in the paper

Acknowledgments

This work was funded by the National Natural Science Foundation of China (No. 52208116) and the China Postdoctoral Science Foundation (No. 2020M681347).

References

- [1] U. Amin, M.J. Hossain, E. Fernandez, Optimal price based control of HVAC systems in multizone office buildings for demand response, *J. Clean. Prod.* 270 (2020), 122059, <https://doi.org/10.1016/j.jclepro.2020.122059>.
- [2] Z. Dalala, Increased Renewable Energy Penetration in National Electrical Grids Constraints and Solutions, *M. Al*, 2022, p. 14.
- [3] Y. Chen, P. Xu, J. Gu, F. Schmidt, W. Li, Measures to improve energy demand flexibility in buildings for demand response (DR): a review, *Energy Build.* 177 (2018) 125–139.
- [4] F. Ran, D. Gao, X. Zhang, S. Chen, A virtual sensor based self-adjusting control for HVAC fast demand response in commercial buildings towards smart grid applications, *Appl. Energy* 269 (2020), 115103, <https://doi.org/10.1016/j.apenergy.2020.115103>.
- [5] Y. Chen, Z. Chen, P. Xu, W. Li, H. Sha, Z. Yang, et al., Quantification of electricity flexibility in demand response: office building case study, *Energy* 188 (2019), 116054.
- [6] Z. Li, J. Zhang, Data-oriented distributed overall optimization for large-scale HVAC systems with dynamic supply capability and distributed demand response, *Build. Environ.* 221 (2022), 109322, <https://doi.org/10.1016/j.buildenv.2022.109322>.
- [7] J. Niu, Z. Tian, J. Zhu, L. Yue, Implementation of a price-driven demand response in a distributed energy system with multi-energy flexibility measures, *Energy Convers. Manag.* 208 (2020), 112575, <https://doi.org/10.1016/j.enconman.2020.112575>.
- [8] R. Yin, E.C. Kara, Y. Li, N. DeForest, K. Wang, T. Yong, et al., Quantifying flexibility of commercial and residential loads for demand response using setpoint changes, *Appl. Energy* 177 (2016) 149–164, <https://doi.org/10.1016/j.apenergy.2016.05.090>.
- [9] H. Wang, S. Wang, A hierarchical optimal control strategy for continuous demand response of building HVAC systems to provide frequency regulation service to smart power grids, *Energy* 230 (2021), 120741, <https://doi.org/10.1016/j.energy.2021.120741>.
- [10] R. Yin, P. Xu, M.A. Piette, S. Kiliccote, Study on Auto-DR and pre-cooling of commercial buildings with thermal mass in California, *Energy Build.* 42 (2010) 967–975, <https://doi.org/10.1016/j.enbuild.2010.01.008>.
- [11] Y. Cao, J. Du, E. Soleymanzadeh, Model predictive control of commercial buildings in demand response programs in the presence of thermal storage, *J. Clean. Prod.* 218 (2019) 315–327, <https://doi.org/10.1016/j.jclepro.2019.01.266>.
- [12] S. Baldi, S. Yuan, P. Endel, O. Holub, Dual estimation: constructing building energy models from data sampled at low rate, *Appl. Energy* 169 (2016) 81–92, <https://doi.org/10.1016/j.apenergy.2016.02.019>.
- [13] Z. Vana, J. Cigler, J. Široký, E. Žáčeková, L. Ferkl, Model-based energy efficient control applied to an office building, *J. Process Control* 24 (2014) 790–797, <https://doi.org/10.1016/j.jprocont.2014.01.016>.
- [14] S. Yang, M.P. Wan, W. Chen, B.F. Ng, D. Zhai, An adaptive robust model predictive control for indoor climate optimization and uncertainties handling in buildings, *Build. Environ.* 163 (2019), 106326, <https://doi.org/10.1016/j.buildenv.2019.106326>.
- [15] S. Bengea, V. Adetola, K. Kang, M.J. Liba, D. Vrabie, R. Bitmead, et al., Parameter estimation of a building system model and impact of estimation error on closed-loop performance, in: 2011 50th IEEE Conference on Decision and Control and European Control Conference, 2011, pp. 5137–5143, <https://doi.org/10.1109/CDC.2011.6161302>.
- [16] J. Arroyo, F. Spiessens, L. Helsen, Identification of multi-zone grey-box building models for use in model predictive control, *Journal of Building Performance Simulation* 13 (2020) 472–486, <https://doi.org/10.1080/19401493.2020.1770861>.
- [17] J. Hu, P. Karava, A state-space modeling approach and multi-level optimization algorithm for predictive control of multi-zone buildings with mixed-mode cooling, *Build. Environ.* 80 (2014) 259–273, <https://doi.org/10.1016/j.buildenv.2014.05.003>.
- [18] J. Chen, G. Augenbroe, X. Song, Lighted-weighted model predictive control for hybrid ventilation operation based on clusters of neural network models, *Autom. ConStruct.* 89 (2018) 250–265, <https://doi.org/10.1016/j.autcon.2018.02.014>.
- [19] P.-D. Morosan, R. Bourdais, D. Dumur, J. Buisson, Building temperature regulation using a distributed model predictive control, *Energy Build.* 42 (2010) 1445–1452, <https://doi.org/10.1016/j.enbuild.2010.03.014>.
- [20] F. Pallonetto, M. De Rosa, F. Milano, D.P. Finn, Demand response algorithms for smart-grid ready residential buildings using machine learning models, *Appl. Energy* 239 (2019) 1265–1282, <https://doi.org/10.1016/j.apenergy.2019.02.020>.
- [21] M. Killian, B. Mayer, M. Kozeck, Effective fuzzy black-box modeling for building heating dynamics, *Energy Build.* 96 (2015) 175–186, <https://doi.org/10.1016/j.enbuild.2015.02.057>.
- [22] A. Aswani, N. Master, J. Taneja, D. Culler, C. Tomlin, Reducing transient and steady state electricity consumption in HVAC using learning-based model-predictive control, *Proc. IEEE* 100 (2012) 240–253, <https://doi.org/10.1109/JPROC.2011.2161242>.
- [23] S. Yang, M.P. Wan, W. Chen, B.F. Ng, S. Dubey, Model predictive control with adaptive machine-learning-based model for building energy efficiency and comfort optimization, *Appl. Energy* 271 (2020), 115147, <https://doi.org/10.1016/j.apenergy.2020.115147>.
- [24] M. Hu, Price-responsive model predictive control of floor heating systems for demand response using building thermal mass, *Appl. Therm. Eng.* (2019) 14.
- [25] H. Viot, A. Sempey, L. Mora, J.C. Batsale, J. Malvestio, Model predictive control of a thermally activated building system to improve energy management of an experimental building: Part I—modeling and measurements, *Energy Build.* 172 (2018) 94–103, <https://doi.org/10.1016/j.enbuild.2018.04.055>.
- [26] J. Gao, T. Yan, T. Xu, Z. Ling, G. Wei, X. Xu, Development and experiment validation of variable-resistance-variable-capacitance dynamic simplified thermal models for shape-stabilized phase change material slab, *Appl. Therm. Eng.* 146 (2019) 364–375, <https://doi.org/10.1016/j.applthermaleng.2018.09.124>.
- [27] S.F. Fux, EKF based self-adaptive thermal model for a passive house, *Energy Build.* 7 (2014).
- [28] T. Berthou, P. Stabat, R. Salvazet, D. Marchio, Development and validation of a gray box model to predict thermal behavior of occupied office buildings, *Energy Build.* 74 (2014) 91–100, <https://doi.org/10.1016/j.enbuild.2014.01.038>.
- [29] J. Zhuang, Y. Chen, X. Chen, A new simplified modeling method for model predictive control in a medium-sized commercial building: a case study, *Build. Environ.* 127 (2018) 1–12, <https://doi.org/10.1016/j.buildenv.2017.10.022>.
- [30] K. Zhang, A. Prakash, L. Paul, D. Blum, P. Alstone, J. Zoellick, et al., Model predictive control for demand flexibility: real-world operation of a commercial building with photovoltaic and battery systems, *Advances in Applied Energy* 7 (2022), 100099, <https://doi.org/10.1016/j.adopen.2022.100099>.
- [31] D. Sturzenegger, D. Gyalistras, M. Morari, R.S. Smith, Model predictive climate control of a Swiss office building: implementation, results, and cost-benefit analysis, *IEEE Trans. Control Syst. Technol.* 24 (2016) 1–12, <https://doi.org/10.1109/TCST.2015.2415411>.
- [32] E. Zacekova, Z. Vana, J. Cigler, Towards the real-life implementation of MPC for an office building: identification issues, *Appl. Energy* 135 (2014) 53–62, <https://doi.org/10.1016/j.apenergy.2014.08.004>.
- [33] S. Zhan, A. Chong, Data requirements and performance evaluation of model predictive control in buildings: a modeling perspective, *Renew. Sustain. Energy Rev.* 142 (2021), 110835, <https://doi.org/10.1016/j.rser.2021.110835>.
- [34] J. Seo, S. Kim, S. Lee, H. Jeong, T. Kim, J. Kim, Data-driven approach to predicting the energy performance of residential buildings using minimal input data, *Build. Environ.* 214 (2022), 108911, <https://doi.org/10.1016/j.buildenv.2022.108911>.
- [35] Y. Chen, M. Guo, Z. Chen, Z. Chen, Y. Ji, Physical energy and data-driven models in building energy prediction: a review, *Energy Rep.* (2022) 16.
- [36] I. Antonopoulos, V. Robu, B. Courraud, D. Kirli, S. Norbu, A. Kiprakis, et al., Artificial intelligence and machine learning approaches to energy demand-side response: a systematic review, *Renew. Sustain. Energy Rev.* 130 (2020), 109899, <https://doi.org/10.1016/j.rser.2020.109899>.
- [37] D. Picard, J. Drgona, M. Kvasnica, L. Helsen, Impact of the controller model complexity on model predictive control performance for buildings, *Energy Build.* 152 (2017) 739–751, <https://doi.org/10.1016/j.enbuild.2017.07.027>.
- [38] Y. Zong, G.M. Boning, R.M. Santos, S. You, J. Hu, X. Han, Challenges of implementing economic model predictive control strategy for buildings interacting with smart energy systems, *Appl. Therm. Eng.* 114 (2017) 1476–1486, <https://doi.org/10.1016/j.applthermaleng.2016.11.141>.
- [39] H. Lee, Y. Heo, Simplified data-driven models for model predictive control of residential buildings, *Energy Build.* 265 (2022), 112067, <https://doi.org/10.1016/j.enbuild.2022.112067>.
- [40] Z. Chen, F. Xiao, F. Guo, J. Yan, Interpretable machine learning for building energy management: A state-of-the-art review, *Advances in Applied Energy* 9 (2023) 100123, <https://doi.org/10.1016/j.adopen.2023.100123>.
- [41] S. Demir, K. Mincev, K. Kok, N.G. Paterakis, Data augmentation for time series regression: applying transformations, autoencoders and adversarial networks to electricity price forecasting, *Appl. Energy* 304 (2021), 117695, <https://doi.org/10.1016/j.apenergy.2021.117695>.
- [42] Z. Wang, T. Hong, Reinforcement learning for building controls: the opportunities and challenges, *Appl. Energy* 269 (2020), 115036, <https://doi.org/10.1016/j.apenergy.2020.115036>.
- [43] M. Raissi, P. Perdikaris, G.E. Karniadakis, Physics-informed neural networks: a deep learning framework for solving forward and inverse problems involving nonlinear partial differential equations, *J. Comput. Phys.* 378 (2019) 686–707, <https://doi.org/10.1016/j.jcp.2018.10.045>.
- [44] G.E. Karniadakis, I.G. Kevrekidis, L. Lu, P. Perdikaris, S. Wang, L. Yang, Physics-informed machine learning, *Nat Rev Phys* 3 (2021) 422–440, <https://doi.org/10.1038/s42254-021-00314-5>.
- [45] J. Zhang, X. Zhao, Three-dimensional spatiotemporal wind field reconstruction based on physics-informed deep learning, *Appl. Energy* 300 (2021), 117390, <https://doi.org/10.1016/j.apenergy.2021.117390>.
- [46] J. Drgona, A.R. Tuor, V. Chandan, D.L. Vrabie, Physics-constrained deep learning of multi-zone building thermal dynamics, *Energy Build.* 243 (2021), 110992, <https://doi.org/10.1016/j.enbuild.2021.110992>.
- [47] G. Gokhale, B. Claessens, C. Develder, Physics informed neural networks for control oriented thermal modeling of buildings, *Appl. Energy* 314 (2022), 118852, <https://doi.org/10.1016/j.apenergy.2022.118852>.
- [48] Y. Li, Z. O'Neill, L. Zhang, J. Chen, P. Im, J. DeGraw, Grey-box modeling and application for building energy simulations - a critical review, *Renew. Sustain. Energy Rev.* 146 (2021), 111174, <https://doi.org/10.1016/j.rser.2021.111174>.
- [49] S. Naderi, G. Pignatta, S. Heslop, I. MacGill, D. Chen, Demand response via pre-cooling and solar pre-cooling: a review, *Energy Build.* 272 (2022), 112340, <https://doi.org/10.1016/j.enbuild.2022.112340>.
- [50] Y. Chen, P. Xu, Z. Chen, H. Wang, H. Sha, Y. Ji, et al., Experimental investigation of demand response potential of buildings: combined passive thermal mass and active storage, *Appl. Energy* 280 (2020), 115956, <https://doi.org/10.1016/j.apenergy.2020.115956>.
- [51] L. Xu, M. Hu, C. Fan, Probabilistic electrical load forecasting for buildings using Bayesian deep neural networks, *J. Build. Eng.* 46 (2022), 103853, <https://doi.org/10.1016/j.jobc.2021.103853>.

- [52] T. Ahmad, H. Zhang, B. Yan, A review on renewable energy and electricity requirement forecasting models for smart grid and buildings, *Sustain. Cities Soc.* 55 (2020), 102052, <https://doi.org/10.1016/j.scs.2020.102052>.
- [53] Y. Lu, Z. Ma, P. Zou, *Heating, Ventilation and Air Conditioning (In Chinese)*, China building industry press, Beijing, 2014.
- [54] Y. Chen, L. Zhang, P. Xu, A. Di Gangi, Electricity demand response schemes in China: pilot study and future outlook, *Energy* 224 (2021), 120042, <https://doi.org/10.1016/j.energy.2021.120042>.